THE JOURNAL OF PHYSICAL CHEMISTRY B LETTERS

2006, *110,* 4503−4505
Published on Web 02/21/2006

Electron Density Redistribution Accounts for Half the Cooperativity of α Helix Formation

Alexandre V. Morozov,[†] Kiril Tsemekhman,[‡] and David Baker*[,§]

Center for Studies in Physics and Biology, The Rockefeller University, 1230 York Avenue, New York, New York 10021, Department of Chemistry, University of Washington, Box 351700, Seattle, Washington 98195, and Department of Biochemistry, University of Washington, Box 357350, Seattle, Washington 98195

Received: December 8, 2005; In Final Form: January 25, 2006

The energy of α helix formation is well known to be highly cooperative, but the origin and relative importance of the contributions to helical cooperativity have been unclear. Here we separate the energy of helix formation into short range and long range components by using two series of helical dimers of variable length. In one dimer series two monomeric helices interact by forming hydrogen bonds, while in the other they are coupled only through long range, primarily electrostatic interactions. Using Density Functional Theory, we find that approximately half of the cooperativity of helix formation is due to electrostatic interactions between residues, while the other half is due to nonadditive many-body effects brought about by redistribution of electron density with helix length.

Alpha helix formation in the gas phase is highly cooperative: the energy per residue increases with increasing helix length.[1] Understanding the nature of α helical cooperativity is important from both conceptual and practical points of view: in order to model cooperative energetics with empirical models one needs to know the relative importance of the underlying physical effects. While cooperativity in α helices,[1] multiply stranded β sheets,[2] and clusters of small molecules[3] has been previously documented in the literature, the origin of α helix cooperativity and the relative magnitude of the many-body, nonadditive contribution have not been quantitatively analyzed.

The increase in the energy per residue with helix length can be decomposed into two parts: first, the increase in the favorable long-range, primarily dipole−dipole electrostatic interactions (Scheme 1; $E_{LR}(n)$), as more residues become available to interact with; and second, the increase in the strength of the short-range interactions (Scheme 1; $E_{SR}(n)$) due to the electron density redistribution with length which acts to enhance intrahelical hydrogen bonds. The relative contributions of these two effects have not been quantitatively decomposed in previous studies.

Here we separate the short- and long-range contributions to helix cooperativity by studying the dimerization energy of a short probe helix with another helix of variable length (Figure 1 and Scheme 1). In one series of helical models (P−NC_n) the probe helix (P) is hydrogen bonded to the main helix (NC_n), with both molecules sharing a common helical axis. Stronger short-range interactions brought about by electron density redistribution with length will be manifested in the strengths of the two interhelical hydrogen bonds. In the other series (P−C_n), the residues in the longer helix that hydrogen bond to the probe are removed and hence long-range electrostatic interactions become dominant. We compute the dimerization energies for both series of models as the difference between the absolute

SCHEME 1: Schematic Representation of α Helical Dimers and Dimerization Energies[a]

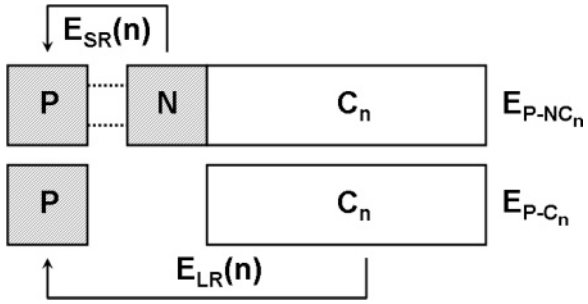

[a] E_{P-NC_n} is the dimerization energy with the hydrogen bonded helix; E_{P-C_n} is the dimerization energy with the helix from which two hydrogen bonded ALA residues are removed. $E_{LR}(n) = E_{P-C_n}$ is the long range contribution to the total dimerization energy; $E_{SR}(n) = E_{P-NC_n} - E_{P-C_n}$ is the short range contribution to the total dimerization energy. NC_n represents a helix with $n + 2$ residues. Two hydrogen bonds between the probe and the main helix are shown as dashed lines.

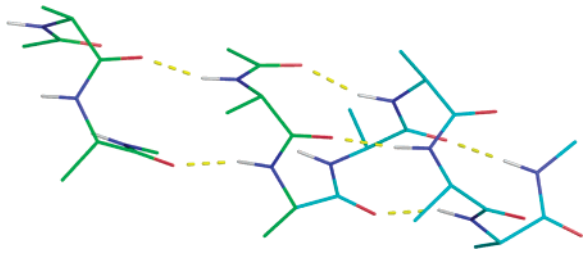

Figure 1. Structural model of the dimer between the probe helix and the 6-residue main helix, with hydrogen bonds shown in yellow. Carbon atoms are colored green if a residue belongs to P or N, and cyan if a residue belongs to C_n. Aliphatic hydrogen atoms are not shown. P, N, and C_n are as defined in Scheme 1.

* Corresponding author. E-mail: dabaker@u.washington.edu.
[†] The Rockefeller University.
[‡] Department of Chemistry, University of Washington.
[§] Department of Biochemistry, University of Washington.

10.1021/jp057161f CCC: $33.50

energy of the dimer and the sum of the absolute energies of the isolated monomers: $E_d = E(AB) - E(A) - E(B)$.

The two contributions to helix cooperativity described above can be separated using the length dependence of these dimerization energies. The long-range contribution, $E_{LR}(n)$, is given directly by E_{P-C_n}, as the short-range interactions are absent by construction. The short-range contribution, $E_{SR}(n)$, is obtained by subtracting this long-range contribution from the dimerization energy of the hygrogen bonded dimers: $E_{SR}(n) = E_{P-NC_n} - E_{P-C_n}$.

The probe molecule has two ALA residues, while the main helices range from 2 to 12 ALA residues in length. Termini are capped with acetyl and *N*-methylamide groups (ACE−ALA_n−NME). All helical models have ideal geometries with standard AMBER98 bond lengths and bond angles.[4] The backbone torsional angles are set to $\phi = -57°$, $\psi = -47°$. Ideal geometries provide the simplest system to study the origins of cooperativity in α helical energies. Single-point dimerization energies are computed using plane wave Density Functional Theory (DFT) with the PW91 exchange-correlation functional and Vanderbilt ultrasoft pseudopotentials as implemented in the VASP software (http://cms.mpi.univie.ac.at/vasp/vasp). This and other DFT exchange-correlation functionals have been shown to reproduce hydrogen bonding and conformational energies obtained through other ab initio methods and experiments with high accuracy.[1e,3f,5] To test the accuracy of our plane-wave PW91 approach, we computed hydrogen bonding energies of several small molecule dimers and compared them with the energies obtained using a local basis set (aug-cc-pV[D,T,Q]Z) with the hybrid B3LYP exchange-correlation functional.[6] The hydrogen bonding energies were very close to each other for all molecules (data not shown). Since plane-wave DFT calculations are of inherently periodic nature, each helical model was placed in a box of the size larger than the dimensions of the molecule and replicated periodically through space. Convergence with respect to the box size and the number of plane waves was explicitly tested in each case. We contrast these DFT energies with pairwise additive energies obtained using the nonpolarizable AMBER98 molecular mechanics (MM) force field[4] implemented in the TINKER 4.0 molecular modeling package[7] (http://dasher.wustl.edu/tinker). AMBER98 is used here to facilitate the study of nonadditive effects captured by the more accurate DFT description. While both Lennard-Jones and Coulomb interactions contribute to the magnitude of MM dimerization energies, the chain length dependence of the helix dimerization energy is dominated by long-range electrostatic effects.

Using dimer models shown in Figure 1 and Scheme 1, we compute the dimerization energy E_{P-NC_n} of the probe molecule with the main *n* residue α helix (which involves formation of two hydrogen bonds) and compare it with the relative energy of adding two residues to a monomeric α helix: $E_{NC_{n+2}} - E_{NC_n}$. While the absolute interaction energies of the probe with the main helix differ from those between residues in a connected helix due to the absence of covalent connectivity, the change in the interaction energy with increase in the helix length is quite similar (Figure 2a, compare black and blue lines). This result justifies our use of helix dimers to study cooperativity in the energies of monomeric helices, and is perhaps not surprising as the strength of the covalent bonds is likely to be much less sensitive to the effects of distant residues than are long range electrostatic and hydrogen bonding interactions. There is a pronounced difference between DFT and pairwise MM energies: the DFT dimerization energy increases by 5.6 kcal/mol between $n = 4$ and $n = 12$, while the corresponding MM energy increases by only 2.4 kcal/mol (Figure 2a).

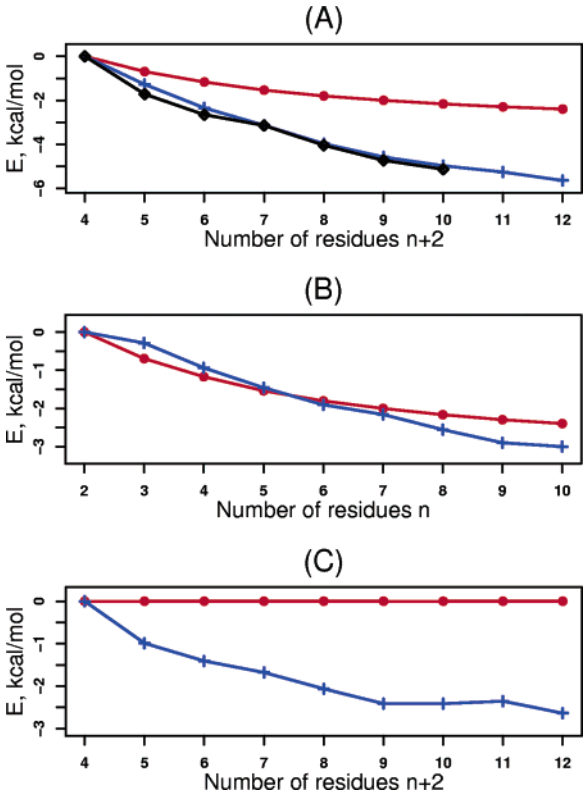

Figure 2. (a) Dimerization energy E_{P-NC_n}. Color scheme: blue (crosses), DFT energies; red (circles), AMBER98 MM energies. Black (diamonds): relative energy of adding 2 residues to a monomeric helix with $n + 2$ residues. (b) The long-range part $E_{LR}(n)$ of the total dimerization energy. (c) The short-range part $E_{SR}(n)$ of the total dimerization energy. All curves are offset to have zero energies at $n = 2$. $n + 2$ is the number of ALA residues in the main helix; *n* is the number of ALA residues in the C_n part of the main helix.

We now proceed to decompose the chain length dependence of the helix dimerization energy into short-range and long-range contributions. To isolate the long-range contribution, we truncate two residues in the main helix that form hydrogen bonds with the probe (Figure 1) and recompute the dimerization energy (E_{P-C_n}). As discussed above, the dimerization energy is dominated by long-range, primarily electrostatic interactions in this case. As shown in Figure 2b, the DFT dimerization energy increases by 3.0 kcal/mol for the 10-residue helix relative to the 2-residue helix. This increase is captured quite well by the MM force field (2.4 kcal/mol), consistent with the expectation that two helices not forming interhelical hydrogen bonds interact primarily via classical electrostatic interactions.

We now have the total dimerization energy E_{P-NC_n} of the probe hydrogen bonded with a helix, and the contribution to this dimerization energy from the long-range interactions (E_{P-NC_n}). To determine how increases in the main helix length increase the strength of the short range (primarily hydrogen bonding) interactions between the probe helix and the two hydrogen bonding partner residues in the main helix, we plot the difference $E_{SR}(n) = E_{P-NC_n} - E_{P-C_n}$ between the two sets of dimerization energies as a function of the number of residues *n* (Figure 2c). With DFT, the short-range interaction energy increases by 2.6 kcal/mol when *n* goes from 4 to 12. In the MM model, the short-range interactions are independent of *n* as expected, since the force field is pairwise additive and the atom pairs contributing to the short-range interactions are unchanged. This difference in the short-range interaction ener-

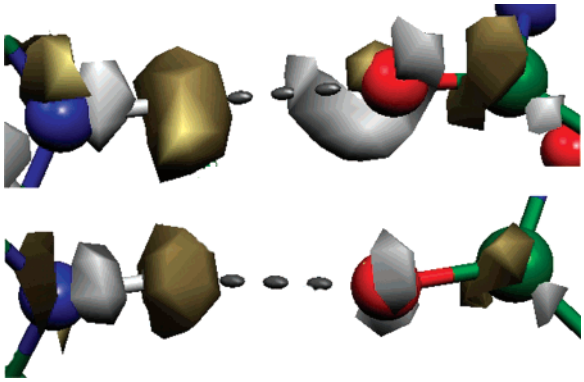

Figure 3. The difference in electron density at the two interhelical hydrogen bonds produced by extending the main helix from $n = 4$ to $n = 7$ ALA residues. Atom color scheme: blue, nitrogen; red, oxygen; green, carbon. Regions where electron density is greater for $n = 7$ are colored in gray; regions depleted in electron density for $n = 7$ are colored in gold. Electron density iso-surfaces correspond to the cutoff of 3×10^{-4}e/a.u.[3]

gies is responsible for the difference in the overall MM and DFT dimerization energies evident in Figure 2a.

The increase in the strength of the short-range interactions may be viewed in terms of hydrogen bonding cooperativity: hydrogen bonds increase in strength due to redistribution of electron density along the helix. We can visualize this effect by plotting electron density contours from the DFT calculation. As shown in Figure 3, there is an increase in electron density around the oxygen and a decrease around the hydrogen with increasing chain length, resulting in stronger hydrogen bonds. We estimate the extent of electron density redistribution associated with the increase in helix length from $n = 4$ to $n = 7$ to be roughly 4% both by directly integrating the electron density around the hydrogen and oxygen atoms and by attributing the change in $E_{SR}(n)$ to the increase in partial charges associated with the two atoms using a simple Coulomb model.

We now return to the question of the origins of cooperativity in α helices. Of the total increase in dimerization energy due to the increase in length of the main helix, 46% (2.6 kcal/mol) is due to the increase in hydrogen bonding strength ($E_{SR}(n)$ in Scheme 1) associated with electron density redistribution, and the rest (3.0 kcal/mol) is due to long-range electrostatic interactions ($E_{LR}(n)$ in Scheme 1). Thus there are two major mechanisms contributing to the cooperativity of α helical energies: long range classical pairwise interactions, and short range nonadditive interactions caused by many-body effects. The contribution of electron density redistribution to cooperativity is significantly higher in α helices than in the formate $-(NMF)_n$ complexes ($n = 2$ to 5),[3j] and in the formamide trimer.[3k] On the other hand, Kobko and Dannenberg estimated the nonpairwise contribution to hydrogen bonding cooperativity to be as high as 75% in long formamide chains.[3b] Because of the many-body effects, nonpolarizable force fields can only very approximately describe helix energetics as they underestimate the cooperativity of α helix formation in the gas-phase by about a factor of two. Reproducing the increase of $E_{SR}(n)$ with helix length will be a good test for the next generation of polarizable force fields. In aqueous solution, both the long-range and short-range interactions will be screened significantly by solvent; defining how this screening affects the balance between the two contributions is an important area for future studies.

Acknowledgment. This work was supported by a fellowship from the Leukemia and Lymphoma Society (to A.V.M.) and by the Howard Hughes Medical Institute (to D.B.). K.T. acknowledges financial support from the Division of Materials Science and Engineering, Office of Basic Energy Sciences, U.S. Department of Energy. The computations were carried out using a grant from the William R.Wiley Environment Molecular Sciences Laboratory, located at the Pacific Northwest National Laboratory.

Supporting Information Available: Cartesian coordinates of all helix dimers used in this study. This material is available free of charge via the Internet at http://pubs.acs.org.

References and Notes

(1) (a) Wu, Y.; Zhao, Y. *J. Am. Chem. Soc.* **2001**, *123*, 5313. (b) Wieczorek, R.; Dannenberg, J. J. *J. Am. Chem. Soc.* **2003**, *125*, 8124. (c) Wieczorek, R.; Dannenberg, J. J. *J. Am. Chem. Soc.* **2003**, *125*, 14065. (d) Wieczorek, R.; Dannenberg, J. J. *J. Am. Chem. Soc.* **2004**, *126*, 14198. (e) Ireta, J.; Neugebauer, J.; Scheffler, M.; Rojo, A.; Galván, M. *J. Phys. Chem. B* **2003**, *107*, 1432. (f) Park, C.; Goddard, W. A., III *J. Phys. Chem. B* **2000**, *104*, 7784.

(2) (a) Zhao, Y.; Wu, Y. *J. Am. Chem. Soc.* **2002**, *124*, 1570. (b) Viswanathan, R.; Asensio, A.; Dannenberg, J. J. *J. Phys. Chem. A* **2004**, *108*, 9205. (c) Horváth, V.; Varga, Z.; Kovács, A. *J. Phys. Chem. A* **2004**, *108*, 6869.

(3) (a) Kobko, N.; Paraskevas, L.; del Rio, E.; Dannenberg, J. J. *J. Am. Chem. Soc.* **2001**, *123*, 4348. (b) Kobko, N.; Dannenberg, J. J. *J. Phys. Chem. A* **2003**, *107*, 10389. (c) Kobko, N.; Dannenberg, J. J. *J. Phys. Chem. A* **2003**, *107*, 6688. (d) Suhai, S. *J. Chem. Phys.* **1994**, *101*, 9766. (e) Suhai, S. *J. Chem. Phys.* **1995**, *103*, 7030. (f) Suhai, S. *J. Phys. Chem.* **1996**, *100*, 3950. (g) Guo, H.; Karplus, M. *J. Phys. Chem.* **1992**, *96*, 7273. (h) Guo, H.; Karplus, M. *J. Phys. Chem.* **1994**, *98*, 7104. (i) Gresh, N. *J. Phys. Chem. A* **1997**, *101*, 8680. (j) Guo, H.; Gresh, N.; Roques, B. P.; Salahub, D. R. *J. Phys. Chem. B* **2000**, *104*, 9746. (k) Mehler, E. L. *J. Am. Chem. Soc.* **1980**, *102*, 4051. (l) Turi, L.; Dannenberg, J. J. *J. Am. Chem. Soc.* **1994**, *116*, 8714.

(4) (a) Cheatham, T. E. III; Cieplak, P.; Kollman, P. A. *J. Biomol. Struct. Dyn.* **1999**, *16*, 845. (b) Cornell, W. D.; Cieplak, P.; Bayly, C. I.; Gould, I. R.; Merz, K. M., Jr.; Ferguson, D. M.; Spellmeyer, D. C.; Fox, T.; Caldwell, J. W.; Kollman, P. A. *J. Am. Chem. Soc.* **1995**, *117*, 5179.

(5) (a) Tuma, C.; Boese, A. D.; Handy, N. C. *Phys. Chem. Chem. Phys.* **1999**, *1*, 3939. (b) Kaschner, R.; Hohl, D. *J. Phys. Chem. A* **1998**, *102*, 5111. (c) Topol, I. A.; Burt, S. K.; Rashin, A. A. *Chem. Phys. Lett.* **1995**, *247*, 112.

(6) Becke, A. D. *J. Chem. Phys.* **1993**, *98*, 5648.

(7) Ponder, J. W.; Richards, F. M. *J. Comput. Chem.* **1987**, *8*, 1016.